# Design of a Tool Integrating Force Sensing with Automated Insertion in Cochlear Implantation

Daniel Schurzig, Robert F. Labadie, Andreas Hussong,
Thomas S. Rau, Robert J. Webster III, *Member, IEEE*

***Abstract*—The quality of hearing restored to a deaf patient by a cochlear implant in hearing preservation cochlear implant surgery (and possibly also in routine cochlear implant surgery) is believed to depend on preserving delicate cochlear membranes while accurately inserting an electrode array deep into the spiral cochlea. Membrane rupture forces, and possibly other indicators of suboptimal placement, are below the threshold detectable by human hands, motivating a force sensing insertion tool. Furthermore, recent studies have shown significant variability in manual insertion forces and velocities, which may explain some instances of imperfect placement. Toward addressing this, an automated insertion tool was recently developed by Hussong et. al. Following the same Insertion Tool Concept, in this paper we present mechanical enhancements that improve the surgeon's interface with the device and make it smaller and lighter. We also present electomechanical design of new components enabling integrated force sensing. The tool is designed to be sufficiently compact and light that it can be mounted to a microstereotactic frame for accurate image-guided pre-insertion positioning. The new integrated force sensing system is capable of resolving forces as small as 0.005N, and we provide experimental illustration of using forces to detect errors in electrode insertion.**

***Index Terms*—Cochlear Implants, Automated Insertion Tool, Force Sensor, Robotic Surgery**

## INTRODUCTION

It has long been recognized that mechatronic technologies can enhance surgical efficacy in applications where small dimensions or complexity of motion are at the border of (or beyond) human manual ability [17]. This is certainly the case in cochlear implant surgery, where both small size and complexity of motion makes deployment of electrodes challenging even for the most experienced surgeons.

D. Schurzig, R. F. Labadie, and R. J. Webster III are with Vanderbilt University, Nashville TN, 37235 USA (phone: (615) 936 2493; fax: (615) 936 5515; e-mail: {daniel.schurzig, robert.labadie, robert.webster} @vanderbilt.edu).

A. Hussong is with Leibniz University Hannover, Germany (andreas.hussong@imes.uni-hannover.de)

Th. S. Rau is with Hannover Medical School, Germany (rau.thomas@mh-hannover.de)

This work was funded in part by the German Research Association (DFG) (MA 4038/1-1, HE-2445/19-1) and the U.S. National Institute of Health under grants R21 EB006044 and R01 DC008408. Some results in this paper have been submitted to the IEEE International Conference on Robotics and Automation, 2010.

Manuscript received December 11, 2009, revised April 16, 2010.

A cochlear implant is a system for artificial sound transduction (see Fig. 1), which restores hearing in patients whose own mechanical-electrical sound transducers (cochlear hair cells) have failed. Generally in such patients, the nerves that form the "wiring" connecting hair cells to the brain's auditory centers are still intact and functional. By directly electrically stimulating these nerves, a cochlear implant restores hearing to an otherwise deaf person.

Modern cochlear implant systems have internal and external components as shown in Fig. 1. The external system senses sound with a microphone, processes it, and transmits wireless signals to an internal receiver/stimulator implanted just under the skin behind the ear. The receiver/stimulator is directly connected by wires to an electrode array inside the cochlea, which stimulates the nerves.

For hearing preservation cochlear implant surgery and potentially all cochlear implant surgery, auditory performance is believed to depend upon sparing intracochlear membranes

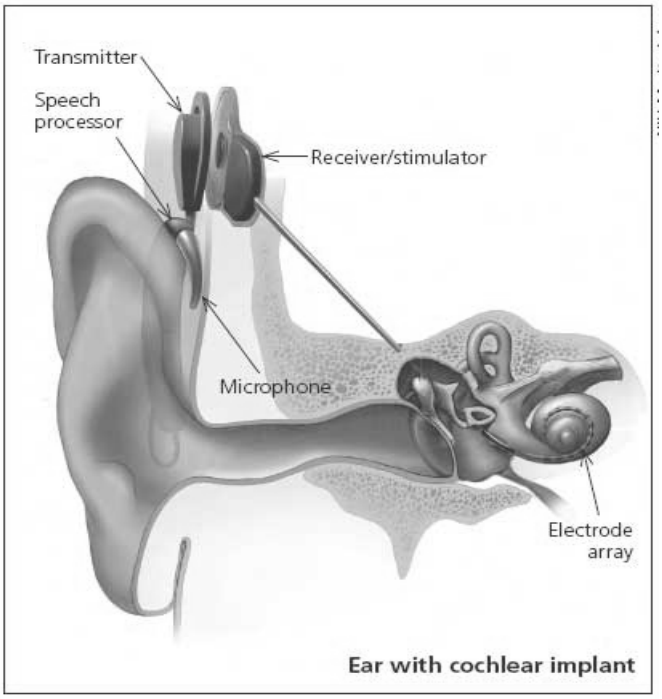


Fig. 1. The human auditory system with a cochlear implant (NIH public domain image). In a healthy person, sound waves entering the ear travel along the ear canal and interact with the eardrum and other mechanical pre-processing structures which convert them to pressure waves in the fluid-filled cochlea. Hair cells convert these waves to electrical impulses which are transmitted to the brain. In patients whose hair cells have ceased to function, a cochlear implant can be used to electrically stimulate the same nerves.

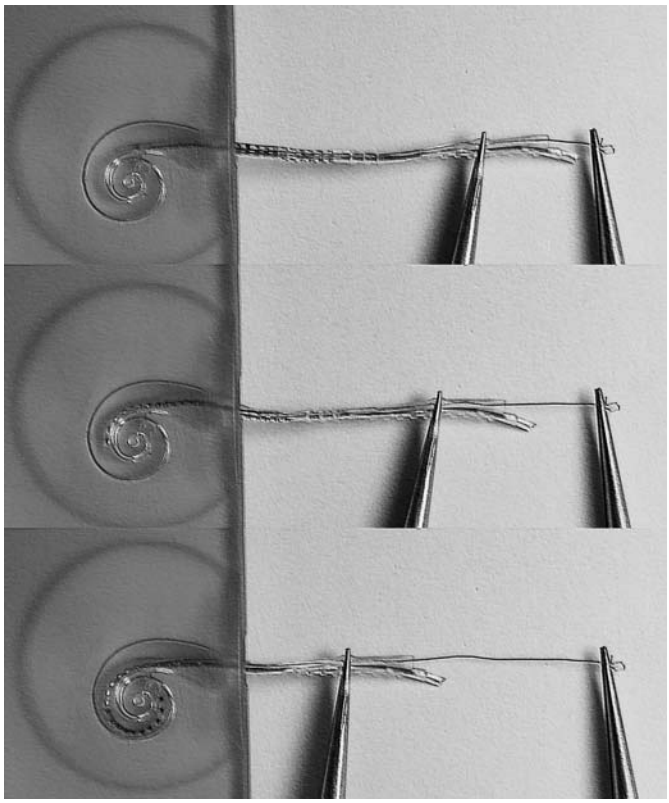

Fig. 2. Cochlear implant electrode insertion involves simultaneously advancing the outer electrode while removing an inner stylet. Shown above is the advance off stylet (AOS) technique for electrode insertion.

while inserting the electrode array [9, 10, 20, 21, 22]. When performed manually, deploying the electrode is challenging. It requires advancement of a 1mm diameter, flexible, curved electrode array into a slightly larger hole in the cochlea—all performed while working down a 15-20mm channel of narrowest width 2mm. To "feel" intracochlear membranes during deployment requires force sensing capabilities beyond the perceptual limits of the human hand. Furthermore, it has recently been shown that the frictional interaction between the electrode and the wall of the cochlea depends on insertion velocity [4], which leads to the hypothesis that repeatable and controllable insertion with real-time force sensing may enable insertion with less damage and better electrode placement than the current manual procedure.

### *A. Optimal Cochlear Implant Positioning*

The best cochlear implant performance (in terms of reducing necessary electrode currents and improving selectivity of nerves excited) is achieved when the electrode array conforms to the helical shape of the cochlea, and rests firmly against the inner wall of the spiral [20, 21]. The importance of optimal electrode placement has led to the recent development of steerable electrode arrays that employ microelectromechanical devices [24], electro active polymers [25], and wire-actuated robotically inserted electrodes [26, 27], all of which are designed to actively control electrode array curvature.

Whether using steerable or traditional electrodes, passing a curved electrode array through a straight access hole and then deploying it into a spiral configuration is challenging. To facilitate this process in a commercially available electrode, the advance off stylet (AOS) insertion technique has been developed (Fig. 2). The electrode array contains a thin straight metal wire – called a stylet – in a channel through its center to keep it straight as it approaches the cochlea. Pulling the stylet out allows the implant to return to its naturally curved shape. During insertion, when the surgeon reaches the point where the electrode array should begin to curve, he/she holds the stylet in position, advancing the silicone electrode array off the sylet. This technique has been shown to reduce the stress on the cochlea during insertion enhancing final array placement [23].

Errors in deployment can occur if the surgeon does not follow this procedure precisely. AOS is challenging to execute due to the small size of the structures involved and the limited access to the surgical site. If the surgeon begins AOS too late, the array will not curl rapidly enough, resulting on increased pressure on sensitive intracochlear structures and potentially incorrect final placement. On the other hand, if the surgeon inadvertently pulls the stylet back during insertion, the array can curl too rapidly and fold over. Both these complications are likely to negatively affect the quality of sound ultimately perceived by the patient. Avoiding these complications and consistently placing electrode arrays at their optimal position motivates the development of an Automated Insertion Tool. In addition to the highly accurate electrode placement, force sensor feedback from our Insertion Tool may indicate impending insertion errors prior to inner ear damage, enhancing safety. An example of deducing the error of beginning AOS too late (that is, too deep) is given in Sec. V. We also explore tip foldover experimentally in Sec V by starting AOS too early (at too shallow a depth).

### *B. Automated Implant Insertion*

In addition to the first prototype Automated Insertion Tool upon which we build in this paper [5, 6], Simaan et al. have developed a mechanism for automated electrode array insertion [4, 26, 27]. They use a single axis insertion robot with an attached axial force sensor for analyzing insertion friction, and up to 4 DoF devices for evaluation of optimal insertion trajectories of their steerable electrode arrays.. While these are promising designs, initial prototypes have been used in benchtop studies primarily aimed at designing better electrode arrays and planning paths for them. Thus some modifications would be needed to adapt the design for use in the operating room under image guidance, as is our objective.

### *C. Contribution*

In this paper our primary contribution is the electromechanical design of an integrated force sensing unit for the Automated Insertion Tool concept of Hussong, et al. [5, 6]. While retaining the basic tool concept, in addition to the force sensor, we also contribute mechanical enhancements that make the Insertion Tool more compact, lighter, and easier to use in the operating room. These mechanical enhancements include an improved Implant Gripper actuated using a knob at the rear of the Insertion Tool, which is easier to access during surgery. We have also redesigned the Front and Base Plates reducing the Insertion Tool weight (important for future

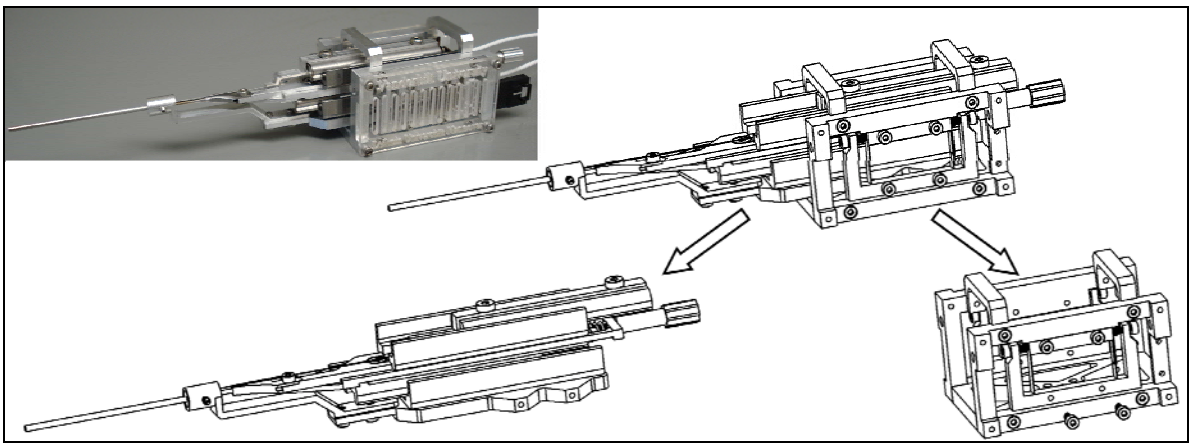

Fig. 3. Insertion Tool Overview showing the two main components (i) Automated Insertion Mechanism (lower left, see also Fig. 4) and (ii) Force Sensing Unit (lower right, see also Fig. 8) described in Sec. IV and V.

integration with a microstereotactic frame), and reduced the diameter of the Guide Tube by more than 50%, which is essential for minimally invasive use of the Tool.

Experimental contributions include (1) verification of sensor performance and linearity, and (2) an experimental illustration of how force information might be used to detect an error in implant insertion, namely the late deployment of the electrode. This is illustrative of how we believe force information will be useful for detecting a wide range of potential placement errors and imperfections in the future. Lastly, we contribute the concept of using an Automated Insertion Tool in conjunction with image-guidance for minimally invasive cochlear implant insertion. This is illustrated in Fig. 14 where we show a conceptual image of the Tool integrated with a microstereotactic frame which is currently undergoing clinical trials at Vanderbilt [13]. For completeness, to illustrate how the force sensor integrates with the Insertion Tool and to illustrate the mechanical similarities and differences between the current prototype and prior prototypes [5, 6], we also provide technical specifications and design sketches for the Insertion Tool.

## II. Tool Concept and Specifications

The Automated Insertion Tool is a compact mechanism that can independently actuate both electrode and stylet, performing programmable insertion profiles including (but not limited to) the AOS technique. To accomplish insertion, one actuator is used to linearly translate the electrode array. A second actuator retracts the stylet during insertion. Both of these actuators provide translational, one degree-of-freedom (DOF) motion.

Technical specifications for the insertion mechanism can be drawn from the physical characteristics of the implant and clinical considerations [6,16]. The length of cochlear implant electrode arrays is 30mm without, and 45mm with, the stylet. We use the Nucleus 24 Contour Advance Electrode from Cochlear Corporation, Inc. in the experimental results presented later in this paper. Electrode array specifications such as these prescribe the necessary travel of the actuators. Since the necessary positioning resolution for optimal electrode placement is not scientifically known, we established this specification at 0.01mm, based on a qualitative estimate by an experienced surgeon. In terms of velocity, our observations of manual insertions reveal an average insertion time of approximately 10 seconds, implying a velocity of 1.8mm/s, given the required insertion depth of 18mm. To permit experimentation with velocities higher than those used manually, we selected 5mm/s as our design target for velocity. Mechanisms must then be attached to each actuator to grip the electrode array and stylet. We choose to grip them in a manner similar to that shown in Fig. 2, but with the forceps oriented so that their shaft is along the electrode axis.

In terms of force sensing requirements, preliminary experiments where the force sensor was mounted beneath cadaver temporal bones indicate that insertion forces are on the order of 0-0.05N and should ideally be measured with a resolution of 0.005N (see [1] for a discussion of these experiments). Experiments and qualitative evaluation by experienced surgeons indicate that a maximum deflection of the insertion tool by 0.5mm is acceptable (to enable force sensing) without hindering electrode deployment.

Using these specifications, the Insertion Tool described in this paper consists of two main modules: (1) the Automated Insertion Mechanism (an enhanced version of the first prototype described in [5, 6]) and (2) the Force Sensing Unit, as shown in Fig. 3. Design of these modules is addressed in the
following two sections.

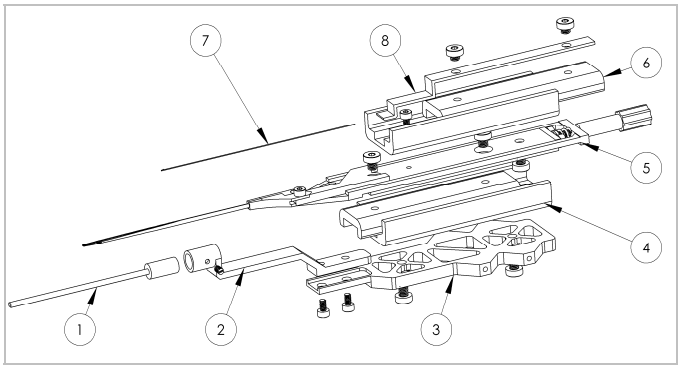


Fig. 4. Exploded view of the Robotic Insertion Mechanism showing (1) the guide tube, (2) the front plate, (3) the base plate, (4) implant gripper actuator, (5) the implant gripper, (6) the stylet hook actuator, (7) the stylet hook, and (8) the gripper.

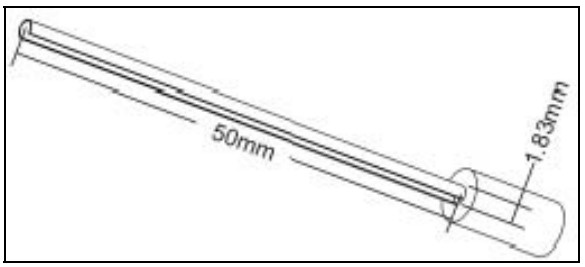


Fig. 5. Close-up of the guide tube which delivers the cochlear implant to the insertion point and houses the implant gripper and stylet hook. The guide tube features a slot which permits the wire attached to the electrode array to connect with the receiver/stimulator shown in Fig. 1.

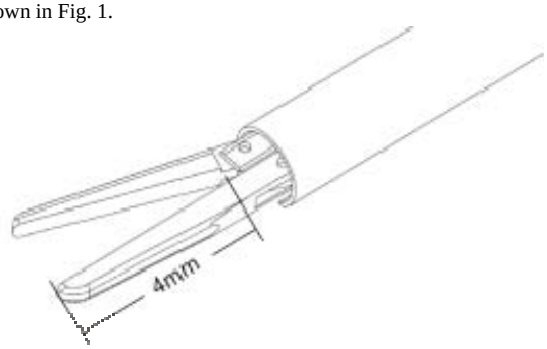


Fig. 6. Tip of the guide tube with forceps of the implant gripper deployed. The gripper holds the base of the cochlear implant and inserts it while the stylet hook (not shown) retracts the stylet during electrode array insertion.

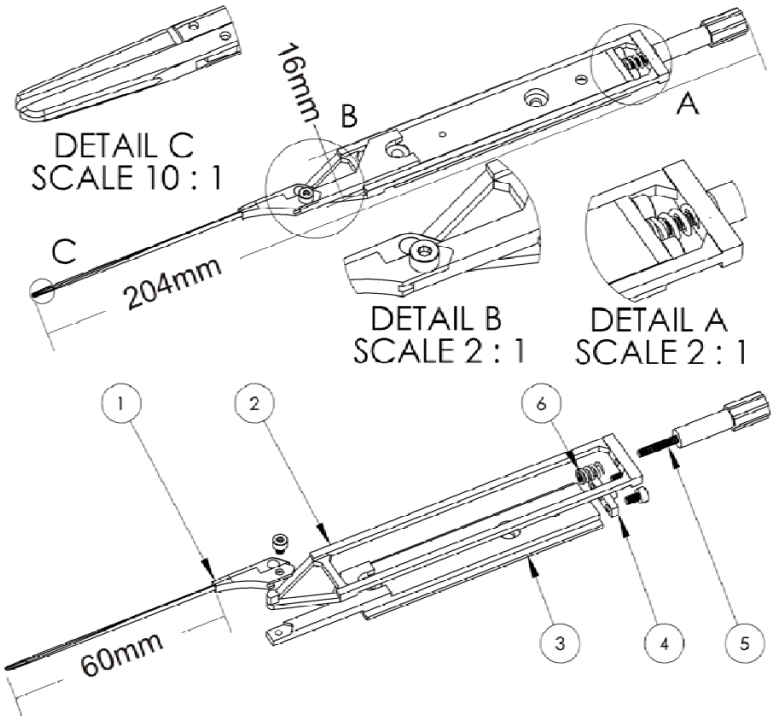


Fig. 7. Implant Gripper showing (1) forceps, (2) slide, (3) middle plate, (4) back plate, (5) adjustment screw, and (6) spring.

## III. Automated Insertion Mechanism Design

An exploded view of the Insertion Mechanism is shown in Fig. 4 and individual components are described below. The most notable enhancement over previously reported mechanisms is the non-backdrivable knob at the back of the device, which controls the gripper that holds the electrode.

The basic concept of the mechanism is as follows. The base (described in Sec. III-A, parts 1 to 3 in Fig. 4), supports a Forceps (which grips the electrode array) that can be inserted and retracted by a linear actuator (Fig. 4, parts 4 and 5). If stylet retraction were not required, these components alone could insert the array. However, in order to retract the sylet components 6, 7 and 8 are mounted on top of part 5. Every movement of the stylet actuator (part 6) is relative to the electrode array linear position.

### *A. Guide Tube, Front Plate, and Base Plate*

As shown on Fig. 3, the structure that holds the insertion mechanism consists of the base and front plates and the guide tube. The tube is connected via the front plate to the base plate which supports the actuators and gripping mechanisms. The guide tube (Fig 5) has an inside diameter of 1.6mm and an outside diameter of 1.83mm, is 60mm long, and is slotted to enable the wires connecting the electrode array to the receiver/stimulator to pass out of it. Within the guide tube are the implant gripper (Sec. III-C) and stylet hook (Sec. III-D). The tip of the guide tube delivers the electrode array to the cochlear entry point. The connection point between the base plate and the Force Sensing Unit (Sec. IV) is via four M2 screws which thread into triangular protrusions on the sides of the base plate (see Figs. 3 and 4).

### *B. Actuators*

The mechanism specifications described in Sec. II require small and high-precision actuators. While it may be possible to design a mechanism meeting all specifications that is actuated by miniature DC motors, since we require linear motions, it is simpler (and likely more compact) to employ linear actuators. This solution has the additional advantage of avoiding gears and hence eliminating possible sources of friction and backlash. Based on these considerations, the insertion tool incorporates *SL-2060* piezoelectric stick-slip linear actuators from SmarAct GmbH (Oldenburg, Germany). These actuators are actuated in sub-nanometer steps and incorporate an internal position sensor that provides displacement resolution of 1μm over 45mm of travel in a package 60mm x 20mm x 10mm. Thus, they meet or exceed all specifications of the Automated Insertion Mechanism.

### *C. Implant Gripper*

The Implant Gripper consists of modified surgical forceps model 180800FX from Fentex medical, Inc. (Neuenhausen ob Eck, Germany). These forceps were selected because of their small diameter, which enables them to fit within a small guide tube (the overall outer diameter of the guide tube must be less than 1.9mm to enable it to pass through a narrow anatomical recess, the facial recess, which is bounded by the Facial Nerve and the Chorda Tympani). An additional advantage of using modified off-the-shelf surgical forceps is their high grip force

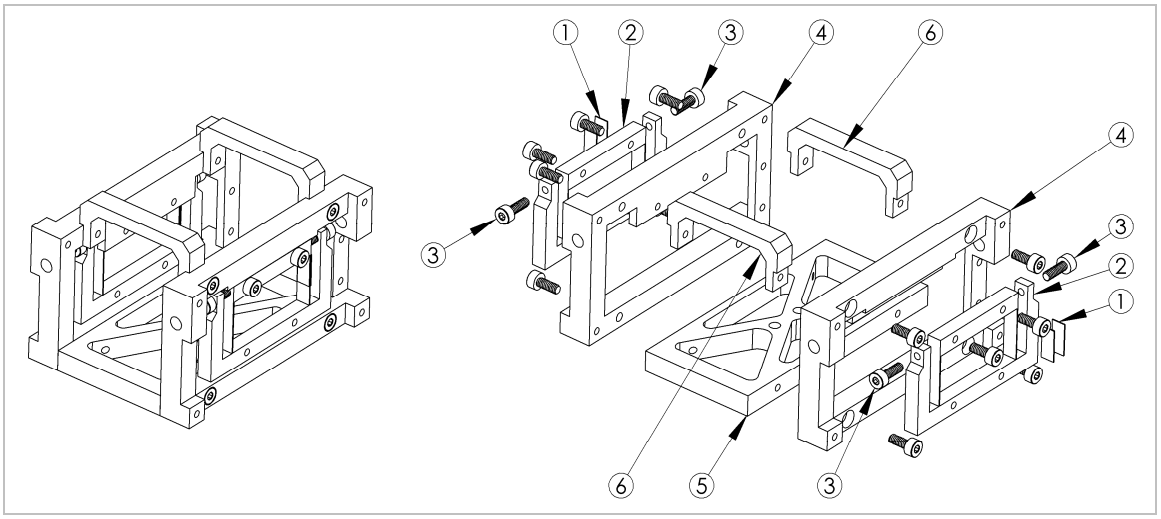


Fig. 8. Force sensing housing. (Left) Assembled, (Right) Exploded view with (1) strain gauges, (2) flexible structure, (3) limit screws, (4) side plates, (5) ground plate, and (6) top bars.

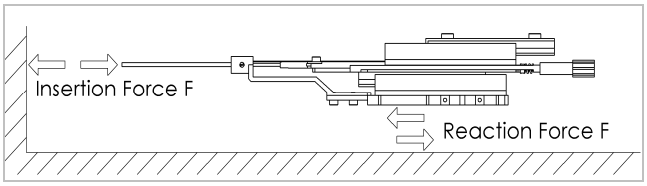


Fig. 9 An insertion force is transmitted through the mechanism and results in a reaction force of the same magnitude on the ground plate.

and stiffness (in comparison to diameter), which are desirable in the insertion tool.

Note that the gripper is able to open far enough to release the implant even when fully retracted within the guide tube. The shaft thickness of the forceps is 2.43mm at its base, and tapers to 1.3mm at its tip. To facilitate loading of the electrode array, the length of the forceps was set (by cutting it to length) so that it extends 5mm beyond the tip of the guide tube when advanced to its forward limit.

To enable easy actuation of the forceps in a compact package, the finger loops were removed in favor of the adjustment screw mounted on the rear of the device as shown in Fig. 7. This screw was designed to be non-backdrivable, so that the forceps will not lose their grip if the physician removes his or her hand from the knob that actuates the adjustment screw. The adjustment screw is a M2 screw threaded into the back plate. The slide is gripped between a shoulder on the screw and the spring, as shown in Fig. 7, and it adjusts the position of the slide relative to the middle plate, which actuates the forceps (Detail B on Fig. 7).

### *D. Stylet Hook*

Since it is necessary for the AOS technique (and other possible insertion techniques) to have independent control of the electrode array and the stylet that straightens it, the insertion tool controls withdrawal of the stylet by means of a Stylet Hook. This hook extends along the Guide Tube parallel to the shaft of the Implant Gripper forceps described above. Whereas the Implant Gripper is mounted on the bottom linear actuator (see Fig. 4), the Stylet Hook is mounted to the top linear actuator. The Stylet Hook is a 0.23mm diameter stainless steel wire with a hook at one end. A hook was

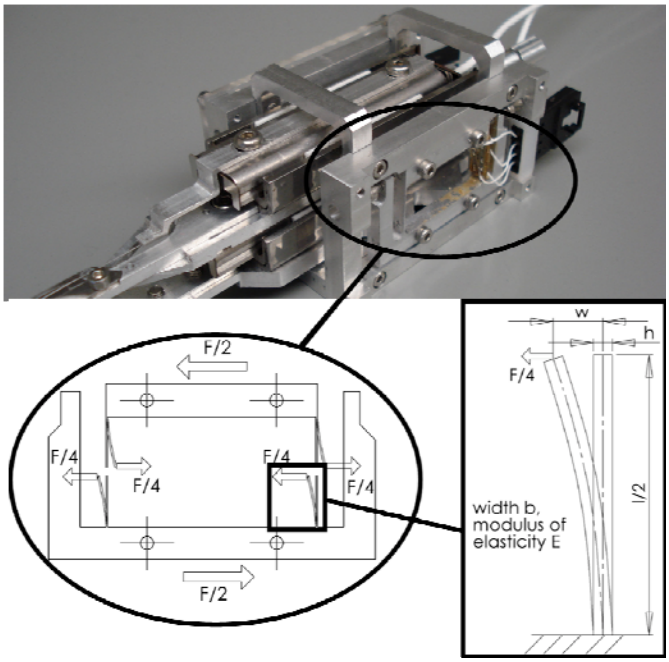


Fig. 10 Side view of the flexible structure indicated in Fig. 8. The beams upon which the strain gauges are mounted deflect under load as shown in the diagram above, enabling force sensing.

selected to manipulate the stylet because its shaft can be very thin, and space within the guide tube is at a premium. The Stylet Hook actuator was mounted on top of the Implant Gripper actuator, such that it controls differential motions between the stylet and electrode array.

## IV. Force Sensing Unit Design

Since intraoperative visualization of the interior of the cochlea is not clinically possible, as discussed in the Introduction, insertion forces can serve as a surrogate indicator of errors in positioning and potential damage to cochlear membranes. In approaching force sensor integration, we began by exploring two two possible sensor placement options. One was to place force sensors within the mechanism itself. For example, one might place one force sensor between the between the Forceps and its linear actuator and a second

between the Stylet Hook and its actuator. Intracochlear forces could then be deduced by subtracting the readings of these two sensors. The disadvantage of this approach is that any friction between interior parts of the insertion mechanism, e.g. Guide Tube and Forceps or Forceps and Stylet Hook, would also appear in measured forces, requiring detailed modeling for compensation (assuming friction forces were repeatable enough that compensation was possible at all).

The other option, which we ultimately pursued, was to measure the reaction forces between the mechanism and the "ground" to which the entire Insertion Tool is attached (see Fig. 9), which removes the friction mentioned above from the measurements. However, a force sensor connected in this way must simultaneously support the weight of the mechanism (leading to a large constant force offset), and measure small intracochlear force signals simultaneously. We were unable to find a commercial force sensor that could meet both these requirements for our insertion tool, motivating our development of a custom solution. The problem with conventional force sensors offering a high resolution such as the *LCL-113G* from *Omega Engineering, Inc*. used in [1] to measure insertion forces by support the cochlea model (not the insertion tool) is that they are typically not able to support significant loads relative to their measurement range, without damage to the sensor.

Thus we chose to design a custom force sensing unit using semiconductor strain gauges rather than the traditional strain gauges (which use resistance changes of thin conductors under load to measure force) included in most commercial force sensors. Semiconductor strain gauges are between 50 and 75 times more sensitive than traditional strain gauges and are significantly more robust – they can generally bend without breaking. The semiconductor strain gauges we chose were four SS-060-033-1000PB from Micron Instruments, Inc. (Simi Valley, CA).

### *A. Basic Concept of Force Sensing Structure*

Our custom force sensing unit (see Figs. 8–10) consists of a collection of thin beams that convert insertion reaction forces into deformations large enough to be measured by strain gauges. While a variety of possible cantilever structures are likely possible for force sensing, we selected the structure shown in Fig. 10. This strategy allows us to design the structure and all dimensions of the force sensing unit precisely to the stiffness and force sensing specifications required in cochlear electrode array insertion. The flexible parts generating a measurable strain are vertical aluminum beams which carry the Insertion Mechanism and are dimensioned to enable them to deflect primarily in the insertion direction, while being relatively resistant to off-axis forces.

### *B. Dimensioning the Flexible Beams*

The core units of the housing are the flexible structures, one of which is shown in Fig. 10. Since there are two copies of this structure (one on each side of the Robotic Insertion Mechanism), the force experienced by each is ½ the insertion force $F$. Since there are two vertical beams (with length $\ell$, height $h$, and width $b$) on each side of the housing, the force is divided by two again such that each strain gauge will measure $F/4$.

To increase their torsional and lateral stiffness as much as possible, the beams' height ($h$) is designed to be small compared to their width ($b$). In order to limit maximum deflection ($w$) mechanically, there are two limit screws per side which set the maximum travel of the larger upright posts shown in Figs. 8 and 10. These are a safety mechanism to prevent over-stressing the force sensing beams. Furthermore, if the limit screws are inserted completely, they make the structure rigid. While this is generally not desirable because it precludes force sensing, it is a useful capability to design into the mechanism in case some specialized future experiments do not require force sensing.

To dimension these force sensing structures, we use the maximum tool tip deflection specification discussed in Section II, namely $w_{\max}$ = 0.5mm. Since the deflection is symmetric, this leads to $w = 0.5 \cdot w_{\max} = 0.25\text{mm}$ for every "half beam" as shown in Fig. 10. To maximize device sensitivity, this deflection should occur when the maximum possible force is applied. This maximum force occurs when the tool is oriented vertically, so that the Guide Tube points downward with respect to gravity. In this configuration the entire mass of the mechanism $m$ = 0.15kg is supported by the beams. Note that we neglect insertion forces in dimensioning beams because they are small relative to device weight. The force supported by each of the four beams is then $F_{\mathrm{B}} = m \cdot g / 4$.

Since the selected semiconductor strain gauges have a width of approximately 3.3mm, the width of the beams was set slightly larger to $b$ = 3.5mm. This allows for gauge installation on the beam face. To keep the dimensions of the overall force sensing housing small, the beam length was set to $\ell$ = 10mm. According to the theory of Bernoulli-Euler beam mechanics (see [2]), the deflection of a beam under a tip load is

$$w = \frac{F_{\mathrm{B}} \cdot \left(\frac{\ell}{2}\right)^3}{3 \cdot E_{\mathrm{Al}} \cdot I}, \qquad (1)$$

where $E_{\mathrm{Al}}$ denotes the elastic modulus of 6061 Aluminum alloy (70GPa), and $I$ is the cross sectional inertia of the beam. Using the $b$ selected above and (1), along with the formula for cross sectional inertia of a rectangular beam ($I = bh^3/12$), one can calculate the required height ($h$) of the beam as approximately 0.15mm. To add an additional safety factor against slightly higher forces than expected, the height of the beam in our prototype was set to 0.2mm. This leads to a deflection of 0.2mm under maximum load, allowing us to sense insertion forces even if they exceed the specification range given in Section II.

### C. *Strain Gauge Circuitry*

As previously mentioned, the force sensor is designed to have a resolution of 5mN while supporting the weight of the insertion mechanism. This requires high sensitivity from strain gauges such as the Micron Instruments semiconductor strain gauges we used. These strain gauges also have significant thermal sensitivity, so we connected them in a full Wheatstone Bridge configuration to compensate. In our implementation two strain gauges are attached via adhesive to each side of each of the flexible beams described in Sec. IV-B above. Amplified strain gauge signals were digitized using an Analog/Digital converter card (DAS16/330, Measurement Computing, Inc., Norton, MA).

## V. Experimental Results

After assembling the tool, it was positioned vertically above a 3D cochlear model manufactured by MED-EL Corporation (Innsbruck, Austria) and a calibration was performed. The first step of this calibration is to define the offset value caused by the weight of the Insertion Mechanism. We did this by performing a force measurement without tool movement. We note that the configuration shown in Fig. 11, where the mechanism is held vertically, represents a worst-case scenario with respect to potential nonlinear effects in our sensor. Thus, it is a good configuration from which to verify linearity in our sensor output. We envision performing this offset subtraction during normal device use in the operating room in the future.


Fig. 11. Experimental setup for experiments using the Insertion Tool to insert an electrode array into a cochlea anatomical model.

Next, to verify measurement accuracy and linearity, known weights are attached to the Insertion Mechanism while recording force measurements. Thus the relationship between the known input force and output voltage of the sensor can be determined and (assuming linearity in response) a constant input multiplication factor can be determined. This procedure was repeated 10 times with increasing and decreasing weight to test the sensor's reliability and hysteresis. The linearity and performance of the force sensor are shown in Fig. 12. The maximum deviation from linearity in the entire calibration range from 0 to 6grams (in steps of 1gram) is 0.003N.

The black profiles in Fig 13 show insertion force results for four insertions of an electrode into a cochlea model using the AOS technique. To interpret the results shown, note that the first 7mm of insertion are the straight insertion, prior to the tip reaching the curved portion of the model shown in Fig. 11. Beginning at 10mm, the retraction of the stylet relative to the electrode array begins, and insertion continues until the tip of the electrode array travels approximately 250° around the

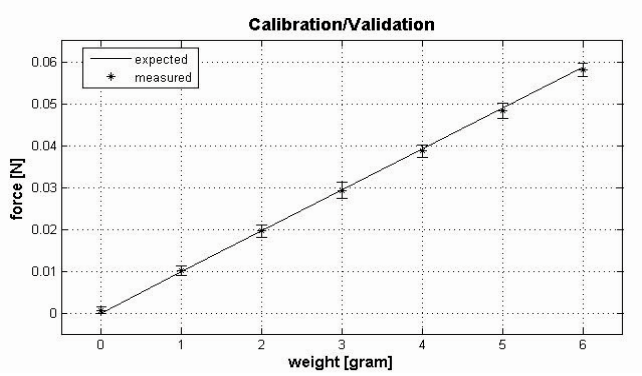


Fig. 12. The above plot shows the forces reported by the force sensor in comparison to the forces applied by hanging known weights from the insertion tool. The largest error across the measurement range was only 0.003N at a weight of 5 grams.

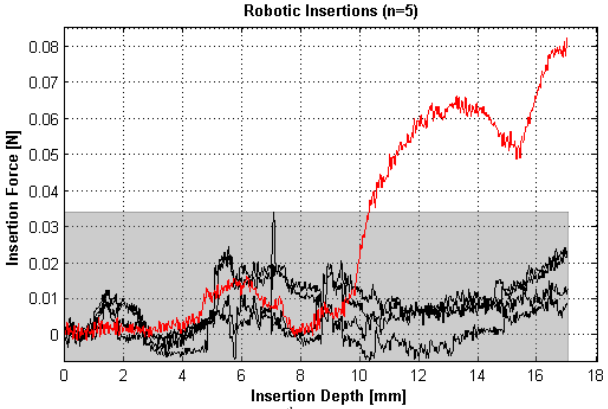


Fig. 13. Filtered Insertion Forces ($5^{th}$ order Butterworth band stop filter, cutoff frequencies $20\text{Hz} \le f_c \le 25\text{Hz}$), recorded with the force sensing Insertion Tool described in this paper. The four black lines represent four successful AOS insertions, whereas the red line shows an insertion without stylet retraction as an example for insertion failure.

cochlea – the desired insertion depth from [1]. Force increases at 5mm insertion depth due to the soft tip of the electrode array touching the medial wall after passing through the cochlear opening (round window). A further description of this phenomenon including image illustration can be found in [5]. We also note that the insertion forces measured with our new device are qualitatively similar to those found with a force sensor mounted to the cochlea model in [1].

The red line in Fig. 13 displays the force resulting from an insertion without stylet retraction. It is clear that a force threshold (such as that indicated by the gray band in the figure) can be used to detect this insertion error. Note that the error could have been detected at a depth of 10.3mm, where the forces first exceed the force threshold, which may permit the insertion to be stopped prior to any potential intracochlear trauma.

The piezoelectric linear actuators in the Automated Insertion Tool introduce noise at 23 Hz with amplitude of approximately 0.02N. To account for this, we filter the raw data using a band-stop filter that attenuates frequencies from 20-25Hz. These values were experimentally determined by examining the difference between force signals when the Insertion Tool was moving and when it was standing still using a Fourier Transform. Thus we attribute them to the actuators or actuator/support structure dynamics. The resulting filtered signal has a signal-to-noise ratio of 4.58, defined by the smallest force difference we desire to measure – 0.005N – divided by the standard deviation of the experimentally measured noise. We note here that the actuators (while having advantages in terms of compactness as discussed in Section II-B) do limit the frequency content of the signals measured. This implies that frequencies in the range of our band-stop filter originating from within the cochlea cannot be measured by the device. This is not an important limitation for exploring current cochlear membrane damage hypotheses, since they consider only the magnitude of applied forces, and not frequency content. Furthermore, because the stop band is small, our device will also be applicable for analysis of dynamic information at a wide range of lower and higher frequencies.

### *A. Tip Foldover Experiment*

To explore the Insertion Tool's ability to sense tip foldover events via force information, we performed an additional experiment. We began AOS at successively shallower depths, starting at the nominal insertion depth of 10 mm. Even beginning AOS at a depth of 3mm (which is beyond the minimum manual error a surgeon would be likely to make), we were unable to create a tip foldover event. This indicates that the repeatability of the Automated Insertion Tool may significantly reduce the incidence of tip foldover, lending support to the idea that a robotic solution may reduce complications in cochlear implantation.

Fig. 14. CAD Drawing of the Automated Insertion Tool we describe in this paper as we envision it being integrated to the Microstereotactic Table developed by Labadie et. al. [9], which we envision providing a means of accurately positioning the insertion tool under image guidance.

## VI. Conclusion and Future Work

In this paper we have described an Automated Insertion Tool for cochlear implant insertion, with mechanical enhancements that make it more compact and easy to use, and the design and application of an integrated force sensor specifically designed for cochlear implantation.

One topic that will be addressed in future work prior to clinical studies with the Automated Insertion Tool is sterilization, and we envision two candidate options. Since the actuators can withstand a maximum temperature of 105°F, and the strain gauge adhesive can withstand 200°F, one possible procedure is to separate the Guide Tube, Front Plate, Forceps and Stylet Hook from the rest of the tool and sterilize those parts alone via steam sterilization (15 minutes at 275°F in an autoclave). However, since time is not an issue and sterilization could be done far in advance to a surgery, gas sterilization of the completely assembled device could also easily be achieved, for example Ethylene Oxide sterilization at 100°F, or possibly Ozone sterilization at 87.4°F to 97°F.

To precisely position the Insertion Tool in-line with the cochlea, we have developed and clinically validated a Microstereotactic Frame [8, 11, 13, 14]. The insertion tool is designed to be mounted on this frame via a custom attachment bracket as shown in Fig 14. In such a configuration our Automated Insertion Tool has the potential to deliver cochlear implants with significantly more repeatable insertion direction

and velocity profiles than is possible using the current manual technique.

Furthermore, the integrated force sensing capability can enhance safety by alerting the physician to placement errors, and possibly even imminent damage to cochlear membranes. An automated mechanism also enables repeatable insertions using a large range of insertion force/velocity/position profiles, including, but not limited to AOS at various velocities. Another technique or profile may ultimately prove most successful in precisely placing cochlear electrodes, while minimizing trauma to the cochlea, and the insertion tool permits rigorous comparison of candidate insertion techniques at various velocities.

The integrated force sensor in the design also enables translation of insertion strategies developed *ex vivo* (with force sensors under the cochlea) into clinical experiments. One future research goal is to use the Insertion Tool in benchtop studies to accurately and repeatably generate placement errors during insertion, analyze their force profiles, and then generate models for error prediction. Our experiments in this paper with tip foldover and excessive insertion depth before stylet retraction provide examples of two possible errors. In the future we believe that force data may also shed light on other more subtle issues such as membrane damage within the cochlea during insertion. Thus, we anticipate that, the force sensing capability of the insertion tool will be useful for fault detection and impending fault detection. In summary, we believe that image-guided cochlear implant insertion with a precise Automated Insertion tool has the potential to enable safer and more accurate cochlear implant insertion, and thus provide better hearing outcomes for patients undergoing cochlear implant surgery.

## REFERENCES


[1] O. Majdani, D. Schurzig, A. Hussong, R. F. Labadie et. al., “Force measurement of insertion of cochlear implants in vitro: comparison of surgeon and automated insertion tool,” in Acta Oto-Laryngologica, 29:1-6, May, 2009.

[2] O. Romberg, N. Hinrichs, translated by J. Steen, J.I. Jenkins, C. Kasperek, “*Don’t Panic with Mechanics!*”. D-65189 Wiesbaden, Germany: Friedr. Vieweg & Sohn Verlag/GWV Fachverlage GmbH, 2005,

[3] J. W. Dally, W. F. Riley, *Experimental Stress Analysis*. Massachusetts, Illinois, Iowa, Wisconsin, New York, California, Missouri: McGraw-Hill, Inc., 1991, ch. 7.

[4] J. Zhang, S. Bhattacharyya, N. Simaan, “Model and Parameter Identification of Friction during Robotic Insertion of Cochlear-Implant Electrode Arrays,” in IEEE *Int. Conf. on Rob. and Aut.*, Kobe, Japan, 2009.

[5] T. S. Rau, A. Hussong, T. Lenarz, O. Majdani et. al., “Automated insertion of performed cochlear implant electrodes: evaluation of curling behaviour and insertion forces on an artificial cochlear model,” *Int.J CARS*, March 2009.

[6] A. Hussong, T. S. Rau, O. Majdani et. al., “An automated insertion tool for cochlear implants: another step towards atrtaumatic cochlear implant surgery,” *Int. J CARS*, May 2009.

[7] A. Jäger, J. Kiefer, W.-D. Baumgartner, C. Jolly, “Cochlear Implant Electrode Design ands Preservation of Residual Hearing”, *7th International Cochlear Implant Conference*, Manchester, UK, 2002.

[8] R. F. Labadie, J. Mitchell, R. Balachandran, J. M. Fitzpatrick, “Customized, Rapid-Production Microstereotactic Table for Surgical Targeting: Description of concept and In-Vitro Validation”, Int. Journal of Computer Assisted Radiology and Surgery, 4(3), 273-280, May 2009.

[9] M. W. Skinner, T. A. Holden, B. R. Whiting, C. C. Finley et. al., “In Vivo Estimates of the Position of Advanced Bionics Electrode Arrays in the Human Cochlea”, in Annals of Otology, Rhinology & Laryngology, 116(4)Suppl 197:1-24, 2007.

[10] J. I. Lane, C. L. W. Driscoll, R. J. Witte, E. P. Lindell et. al., “Scalar Localization of the Electrode Array After Cochlear Implantation: A Cadaveric Validation Study Comparing 64-Slice Multidetector Computed Tomography With Microcomputed Tomography”, in Otology & Neurotology, 28:191-194, 2007.

[11] R. Balachandran, O. Majdani, J. Noble, R. F. Labadie et. al., “Percutaneous Cochlear Implant Drilling via Customized Frames”, to be presented at the *AAO-HNSF 2009 Annual Meeting & OTO EXPO*, San Diego, California, October 4-7, 2009.

[12] D. Schurzig, O. Majdani, A. Hussong, R. F. Labadie et. al., “Robotic Insertion of Cochlear Implant Electrode Arrays”, *12th Symposium on Cochlear Implants in Children*, Seattle, Washington, June 17-20, 2009.

[13] Labadie RF, Balachandran R, Mitchell J, Noble JH, Majdani O,Haynes DS, Bennett ML, Dawant BM. Clinical Validation Study of Percutaneous Cochlear Access Using Patient Customized Micro-Stereotactic Frames. Otology & Neurotology 2009 (in press)

[14] F. M. Warren, R. F. Labadie, R. Balachandran, J. M. Fitzpatrick, “Percutaneous Cochlear Access Using Bone-Mounted, Customized Drill Guides: Demonstration of Concept In-Vitro”, 2006 American Otological Society Meeting, Chicago, Illinois, May 20-21, 2006.

[15] C. James, K. Albegger, R. Battmer, N. Dillier et. al., “Preservation of Residual Hearing with Cochlear Implantation: How and Why”, Acta Oto-Laryngologica, 125(5):481-91, May, 2005.

[16] A. Hussong, T. Rau, H. Eilers, S. O. Majdani et. al., “Conception and Design of an Automated Insertion Tool for Cochlear Implants”, in *Conf. Proc. IEEE Eng Med Biol Soc.*, 2008

[17] F. Tendick, S. S. Sastry, R. S. Fearing, M. Cohn, “Applications of micromechatronics in minimally invasive surgery”, IEEE Trans. Mech, vol. 3, pp. 34–42, Mar. 1998.

[18] K. Tanaka, M. Abe, S. Ando, “A novel mechanical cochlea “Fishbone” with dualsensor/actuator characteristics”, IEEE Trans. Mech, vol. 3, pp. 98–105, Jun. 1998.

[19] C. A. Todd, F. Naghdy, M. J. Svehla, “Force Application During Cochlear Implant Insertion: An Analysis for Improvement of Surgeon Technique”, IEEE Trans. Mech, vol. 54, pp. 1247–1255, Jul. 2007.

[20] J. H. M. Frijns, J. J. Briarie, and J. J. Grote, "The Importance of Human Cochlear Anatomy for the Results of Modiolus-Hugging Multi-channel Cochlear Implants," Otology & Neurotology, vol. 22, pp. 340-349, 2001.

[21] R. S. Huang TC, Marrinan MS, Waltzman SB, Roland JT., "Modiolar coiling, electrical thresholds, and speech perception after cochlear implantation using the nucleus contour advance electrode with the advance off stylet technique.," Otol Neurotol., vol. 27, pp. 159-66, 2006 Feb.

[22] C. James, K. Albegger, and R. a. Battmer, "Preservation of residual hearing with cochlear implantation: how and why," Acta Otolaryngol, vol. 125, pp. 481-491, 2005.

[23] T. Roland, "A model for cochlear implant electrode insertion and force evaluation: results with a new electrode design and insertion technique " The Laryngeoscope, vol. 115, pp. 1325-1339, 2005.

[24] J. Wu, L. Yan, H. Xu, W. C. Tang, and F.-G. Zeng, "A curvature-controlled 3D micro-electrode array for cochlear implants," Seoul, South Korea, 2005, pp. 1636-1639.

[25] B. Chen, H. Kha, and G. Clark, "Development of a steerable cochlear implant electrode array," in 3rd Kuala Lumpur International Conference on Biomedical Engineering 2006, 2007607-610.

[26] J. Zhang, K. Xu, N. Simaan, and S. Manolidis, "A Pilot Study of Robot-Assisted Cochlear Implant Surgery Using Steerable Electrode Arrays," in MICCAI'06 - the 9th International Conference on Medical Imaging and Computer-Assisted Intervention Copenhagen, 2006.

[27] J. Zhang, T. J. Roland, S. Manolidis, and N. Simaan, "Optimal Path Planning for Robotic Insertion of Steerable Electrode Arrays in Cochlear Implant Surgery," ASME Journal of Medical Devices, vol. 3, 2009.